



Strain-hardening fiber cement optimization and component tailoring by means of a micromechanical model

En-Hua Yang, Victor C. Li *

Department of Civil and Environmental Engineering, University of Michigan, Ann Arbor, 48109-2125 MI, United States

ARTICLE INFO

Article history:

Available online 23 September 2009

Keywords:

Fiber cement
Composite optimization
Tensile ductility
Polyvinyl alcohol fiber (PVA)
Polypropylene fiber (PP)
Copolymer fiber

ABSTRACT

It is well known that fibers can impart tensile ductility into fiber cement products. Specific rational guideline for engineering desirable fiber, matrix, and interface properties leading to optimized fiber cement product performance; however, is scarce. This paper discusses the theoretical basis for composite optimization of synthetic fiber reinforced cement that leads to maximum tensile ductility while minimizing the content of the expensive fiber component of fiber cement products. Specific tailoring of polyvinyl alcohol (PVA) fiber and polypropylene (PP) fiber and experimentally verified tensile ductility characteristics of the resulting fiber cement products are employed to illustrate the theoretical concepts. It is demonstrated that high product performance can be achieved with minimal amount of fibers via composite optimization. The theoretical tools developed are applicable to a wide range of fiber types and matrix types.

© 2009 Elsevier Ltd. All rights reserved.

1. Introduction

It is well known that fibers are essential for the ductile performance of fiber cement, a composite with a highly brittle matrix. In the past, this ductile performance has been supported by the use of low cost asbestos fiber in relatively large amount, 9–14% by weight [1]. With the world-wide trend of substituting asbestos fiber, the industry is increasingly turning to synthetics. Some synthetic fibers can be relatively expensive, while others appear to limit the composite performance. However, synthetic fibers offer the opportunity for tailoring – in fiber length and diameter, mechanical characteristics, surface treatment, etc. It is only natural, therefore, to ask the question how fiber cement should be designed, so that optimal composite performance is achieved at the lowest cost.

A micromechanical model developed recently at the University of Michigan for randomly oriented discontinuous fiber reinforced brittle matrix composites may shed light on fiber cement optimization. Specifically, this model can be used to address optimal mix composition of fiber, matrix and interface characteristics in order to achieve maximum tensile ductility while minimizing the amount of fiber. Emphasis is placed on the need for a holistic approach in composite design. Further, the model can be used to guide the tailoring of fiber characteristics, including surface treatment, or the tailoring of the matrix composition, including the use of artificial defects.

This paper summarizes the essentials of the micromechanical model based on Li and Leung [2] and Lin et al. [3] but with recent updating by Yang et al. [4], and demonstrates how it guides towards composite optimization. Specific examples are then given of fiber, matrix, and interface tailoring. Special attention is given to polyvinyl alcohol (PVA) fiber as this fiber has been one of the dominant synthetic fibers used in the fiber cement industry, and to polypropylene (PP) fiber which appears to gain increasing acceptance with property improvements in recent years. It is shown that in the case of PVA fiber, surface treatment leading to a reduction of bond properties is beneficial to composite ductility. In contrast, increase in frictional bonding along with fiber strength greatly enhances composite performance when PP fiber is utilized.

2. Micromechanics-based strain-hardening model for randomly oriented discontinuous fiber reinforced brittle matrix composites

The design strategy of strain-hardening fiber reinforced brittle matrix composites lies in realizing and tailoring the synergistic interaction between fiber, matrix, and interface. Micromechanics can be used as a tool to link material microstructures to composite properties. Desirable composite behavior can be tailored by control of material microstructures once the linkages are established.

The pseudo strain-hardening behavior in fiber reinforced brittle matrix composite is achieved by sequential development of matrix multiple cracking. The fundamental requirement for multiple cracking is that steady-state flat crack extension prevails under

* Corresponding author. Tel.: +1 734 764 3368; fax: +1 734 764 4292.
E-mail address: vcli@umich.edu (V.C. Li).

tension, which requires the crack tip toughness J_{tip} to be less than the complementary energy J'_b calculated from the bridging stress σ versus crack opening δ curve, as illustrated in Fig. 1 [5].

$$J_{tip} \leq \sigma_0 \delta_0 - \int_0^{\delta_0} \sigma(\delta) d\delta \equiv J'_b \quad (1)$$

where $J_{tip} = K_m^2/E_m$, σ_0 is the maximum bridging stress corresponding to the opening δ_0 , K_m is the matrix fracture toughness, and E_m is the matrix Young's modulus. Eq. (1) employs the concept of energy balance during flat crack extension between external work, crack tip energy absorption through matrix breakdown (matrix toughness), and crack flank energy absorption through fiber/matrix interface debonding and sliding. This energy-based criterion determines the crack propagation mode (steady-state flat crack or modified Griffith crack). The predominance of flat crack extension over modified Griffith crack propagation is important since the crack width can be constrained to below δ_0 , and the stress level is always maintained below the bridging capacity of the fibers. Otherwise, localization of a fracture will prevail, resulting in tension-softening and large opening of a single crack.

The stress-crack opening relationship $\sigma(\delta)$, which can be viewed as the constitutive law of fiber bridging behavior, is derived by using analytic tools of fracture mechanics, micromechanics, and probabilistics [3]. In particular, the energetics of tunnel crack propagation along fiber/matrix is used to quantify the debonding process and the bridging force of a fiber with given embedment length. Probabilistics is introduced to describe the randomness of fiber location and orientation with respect to a crack plane. The random orientation of fiber also necessitates the accounting of the mechanics of interaction between an inclined fiber and the matrix crack. As a result, the $\sigma(\delta)$ curve is expressible as a function of micromechanics parameters, including interface chemical bond G_d , interface frictional bond τ_0 , and slip-hardening coefficient β accounting for the slip-hardening behavior during fiber pullout. G_d is used to quantify the fracture energy required for interface debonding and τ_0 describes the friction force during sliding. In addition, snubbing coefficient f and strength reduction factor f' are introduced to account for the interaction between fiber and matrix as well as the reduction of fiber strength when pulled at an inclined angle. Besides interfacial properties, the $\sigma(\delta)$ curve is also governed by the matrix Young's modulus E_m , fiber content V_f , and fiber diameter d_f , length L_f , and Young's modulus E_f .

Another condition for the pseudo strain-hardening is that the matrix first cracking strength σ_{fc} must not exceed the maximum fiber bridging strength σ_0 .

$$\sigma_{fc} < \sigma_0 \quad (2)$$

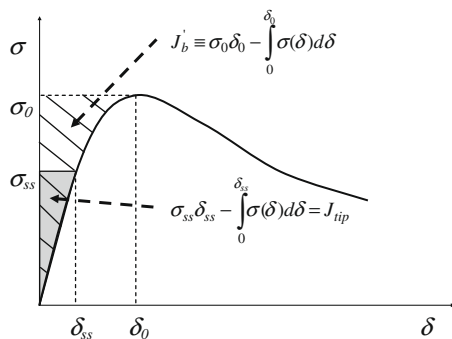


Fig. 1. Typical $\sigma(\delta)$ curve for tensile strain-hardening composite. Hatched area represents maximum complementary energy J'_b . Shaded area represents crack tip toughness J_{tip} .

where σ_{fc} is determined by the matrix fracture toughness K_m , pre-existing internal flaw size a_0 , and the $\sigma(\delta)$ curve. While the energy criterion Eq. (1) governs the crack propagation mode, the strength-based criterion represented by Eq. (2) controls the initiation of cracks. Satisfaction of both Eqs. (1) and (2) is necessary to achieve ductile strain-hardening behavior; otherwise, normal tension-softening FRC behavior results. Details of these micromechanical analyses can be found in previous works [2,3].

Due to the random nature of pre-existing flaw size and fiber distribution in cement composites, a large margin between J'_b and J_{tip} as well as σ_{fc} and δ_0 is preferred. The pseudo strain-hardening (PSH) performance index has been used to quantitatively evaluate the margin and is defined as follows [6]:

$$PSH \text{ energy} = \frac{J'_b}{J_{tip}} \quad (3)$$

$$PSH \text{ strength} = \frac{\sigma_0}{\sigma_{fc}} \quad (4)$$

Materials with larger values of PSH indices should have a better chance of saturated multiple cracking. Unsaturated PSH behavior often leads to small tensile strain capacity and large variability of tensile ductility of the composites. It has been demonstrated experimentally that polyethylene (PE) fiber reinforced cement composites with performance indices $J'_b/J_{tip} > 3$ and $\sigma_0/\sigma_{fc} > 1.2$ produce saturated PSH behavior [6]. However, for the PVA fiber reinforced cement composites, the crack patterns observed required modification of the σ_0/σ_{fc} index to be greater than 1.45 instead of 1.2 [7]. This is due to higher rupture tendency, i.e. lower fiber strength and higher interfacial bonds when compared with PE fiber, for the PVA fiber, which result in larger variation in the bridging capacity, thus requiring higher margin between the first crack and the peak bridging strength. A similar argument applies to the PP fiber reinforced composites. Here, although the interfacial bond properties of PP fiber cement are similar to that of PE fiber cement (due to the hydrophobic surface of both fibers), the fiber strength of PP is much lower than that of PE [6]. In this study, a PSH strength index $\sigma_0/\sigma_{fc} > 2$ is assumed for the PP fiber system. Further experimentally confirmation of this assumption is required. To ensure saturated multiple cracking for the PVA and PP fiber composites, these modified values of performance indices (PSH strength value = 1.45 and 2 for PVA and PP respectively; PSH energy value = 3 for both) will be utilized in the following calculations.

3. Illustration of model-based composite optimization

As described above, the micromechanics-based strain-hardening model links material microstructures and composite behavior and serves as a tool to guide composite optimization through properly tailored fiber, matrix, and interface properties. In this section, illustration of model for composite optimization is described. Focus is placed on thin sheet cement composites reinforced with randomly oriented discontinuous PP fibers or PVA fibers.

Fig. 2 shows the calculated critical fiber volume as a function of interface frictional bond for achieving saturated multiple cracking and tensile strain-hardening behavior of a PP fiber (control PP) reinforced thin sheet cement composite based on the micromechanics model with 2-D fiber orientation assumption. The 2-D fiber orientation assumption is particularly applicable for the thin sheet fiber cement due to process induced fiber layering and sheet thickness smaller than fiber length. The two curves in Fig. 2a, relating V_{crit}^f to τ_0 were calculated by specifying all other micromechanical parameters (Table 1) and plugging them into the strain-hardening criteria, i.e. energy criterion and strength criterion in Eq. (1) and

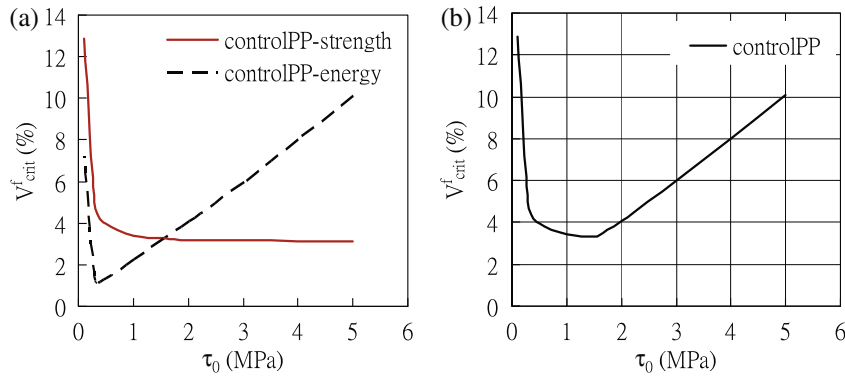


Fig. 2. Micromechanical model calculated V_{crit}^f as a function of τ_0 for strain-hardening (control) PP fiber cement determined by: (a) the energy and the strength criterion respectively and (b) the combined effect.

Table 1

Micromechanical parameters used in calculating V_{crit}^f of PP fiber cement.

	Fiber parameters				Interface parameters				Matrix parameters	Energy criterion		Strength criterion	
	d_f (μm)	L_f (mm)	E_f (GPa)	σ_{fu} (MPa)	G_d (J/m^2)	β	f	f'		E_m (GPa)	J_{tip} (J/m^2)	J_b (J/m^2)	σ_{fc} (MPa)
Control PP	16.6	8	11.6	400	0	0.005	0.39	0.1	20	5	15	2.5	5
LongPP	16.6	19	11.6	400	0	0.005	0.39	0.1	20	5	15	2.5	5
Strong PP	16.6	8	11.6	928	0	0.005	0.39	0.1	20	5	15	2.5	5

(2), respectively. The micromechanical parameters were independently measured or deduced [1,8].

As can be seen from Fig. 2a, V_{crit}^f calculated from the strength criterion approaches a constant at high frictional bond and sharply increases at low frictional bond ($\tau_0 < 0.3$ MPa). The bridging strength is known to be governed by fiber strength, fiber volume, and interfacial properties, e.g. τ_0 and G_d . At higher interfacial friction; however, fiber rupture dominates over fiber pull-out so that the bridging strength becomes insensitive to τ_0 . Because fiber strength is given, fiber volume approaches to a steady value in order to satisfy the strength criterion ($\sigma_o = 5$ MPa). At low friction; however, fiber pull-out prevails over fiber rupture and bridging strength is now insensitive to the fiber strength and governed by fiber volume and τ_0 . High amount of fiber is therefore required to obtain adequate bridging strength of 5 MPa.

Interestingly, a concave V_{crit}^f curve was obtained based on the energy criterion. The energy criterion requires the complementary energy of $\sigma(\delta)$, shaded area in Fig. 1, to reach a specified value ($15 \text{ J}/\text{m}^2$) in order to ensure robust steady-state cracking. In general, the bridging strength decreases with reduction of τ_0 , resulting in low J_b at low τ_0 region. At high τ_0 end, the stiffness of the fiber bridging “springs” (i.e. the initial slope of the $\sigma(\delta)$) keeps rising, resulting in a decrease in J_b also. High fiber fraction is therefore required at both high and low τ_0 in order to satisfy the $15 \text{ J}/\text{m}^2$ complementary energy. An optimum point, i.e. a balanced interfacial friction (τ_0 around 0.25 MPa) which meets the specified J_b at minimum fiber fraction, exists in the energy curve.

Strain-hardening behavior relies on the satisfaction of both the strength and energy criteria. Therefore, the minimum fiber amount to achieve saturated multiple cracking is the combination of the two curves whichever has higher V_{crit}^f as depicted in Fig. 2b. The combined curve shown in Fig. 2b indicates that the optimum point for the strain-hardening behavior of this control PP fiber cement falls in the range of 3.5 vol.% fiber content with 1.5 MPa interface frictional bond strength. However, due to the hydrophobic nature of PP fiber, the interfacial bonds are usually very weak, e.g. $G_d \sim 0 \text{ J}/\text{m}^2$ and τ_0 is usually in the range of 0.2–0.3 MPa [1]. Therefore, much higher fiber content (7–13 vol.%) is usually adopted in ductile PP fiber cement materials [9,10].

Low tensile strength has been recognized as a major drawback of PP fiber. High tenacity PP fiber was therefore developed. Fig. 3 shows the effect of fiber strength on V_{crit}^f versus τ_0 curves. These curves were calculated using the same set of micromechanical parameters as for the control PP fiber, except that the fiber strength was increased to 928 MPa [8]. As can be seen, enhanced fiber strength greatly reduces V_{crit}^f at higher friction ($\tau_0 > 0.3$ MPa) for both the strength and energy curves as well as the combined curve. Meanwhile, for the strong PP case, strength criterion overrides the energy criterion and dominates the combined V_{crit}^f curve in the range of τ_0 from 0 to 5 MPa. For ordinary high tenacity PP fiber with frictional bond between 0.2 and 0.3 MPa; however, V_{crit}^f over 4% is still needed to achieve robust strain-hardening. To take advantage of the improved fiber strength in high tenacity PP fiber, it is also necessary to increase the interface frictional bond τ_0 to around 1 MPa or above. This example underlines the importance of understanding the governing mechanisms through micromechanics-based models in design of ductile composites.

Fig. 4 illustrates the effect of fiber length on the V_{crit}^f curve. All micromechanical parameters used in calculating the long PP fiber case are identical with the control PP fiber except the fiber length is changed from 8 to 19 mm. In contrast to increase of fiber strength, both individual strength- and energy-based curves and the combined curve of long PP fiber drop significantly at the low τ_0 end ($\tau_0 < 1$ MPa) and do not change much when τ_0 is beyond 1 MPa. This calculation indicates that increase of fiber length is especially beneficial for fiber reinforced composite with low interfacial friction in achieving strain-hardening behavior, which is the case for the normal PP fiber cement. However, fiber length may be limited by processing requirements.

PVA fiber featuring high stiffness, high tensile strength, and strong interfacial bonding has been one of the dominant synthetic fibers used in the fiber cement industry. The relative high cost of PVA fiber prohibits usage of high fiber fraction in the cost-sensitive construction industry. Therefore, composite optimization of PVA-fiber cement becomes even more critical and valuable. Table 2 lists the micromechanical parameters used in calculating the V_{crit}^f plots for the PVA-fiber cement [11,12]. The high interface chemical bond $G_d = 5 \text{ J}/\text{m}^2$ measured is due to the hydrophilic nature of virgin PVA

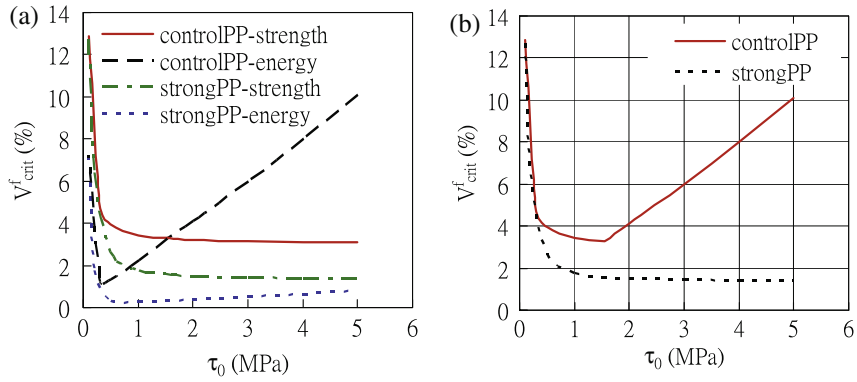


Fig. 3. Effect of fiber strength on V_{crit}^f determined by: (a) the energy and the strength criterion respectively and (b) the combined effect.

Table 2

Micromechanical parameters used in calculating V_{crit}^f of PVA-fiber cement.

	Fiber parameters				Interface parameters				Matrix parameters	Energy criterion		Strength criterion	
	d_f (μm)	L_f (mm)	E_f (GPa)	σ_{fu} (MPa)	G_d (J/m^2)	β	f	f'		E_m (GPa)	J_{tip} (J/m^2)	J'_b (J/m^2)	σ_{fc} (MPa)
G _d 5 PVA	39	12	42.8	1070	5	0.05	0.5	0.32	20	5	15	4.5	6.5
G _d 2PVA	39	12	42.8	1070	2	0.05	0.5	0.32	20	5	15	3.5	5
G _d 2PVA (flaw)	39	12	42.8	1070	2	0.05	0.5	0.32	20	5	15	3.5	4
G _d 2PVA (low J_{tip})	39	12	42.8	1070	2	0.05	0.5	0.32	20	3.3	10	2.5	3.5

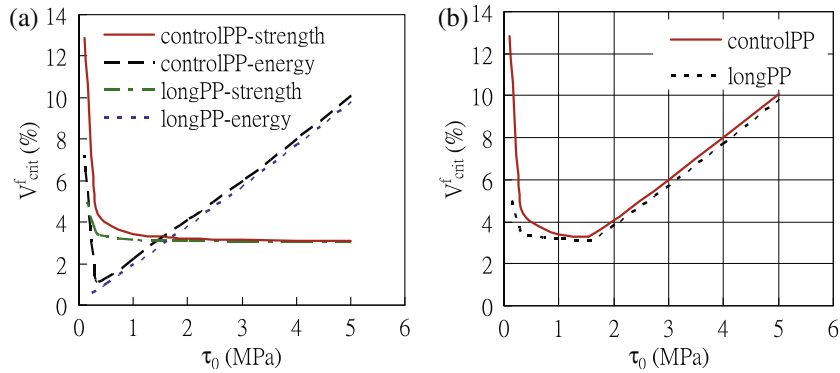


Fig. 4. Effect of fiber length on V_{crit}^f determined by: (a) the energy and the strength criterion respectively and (b) the combined effect.

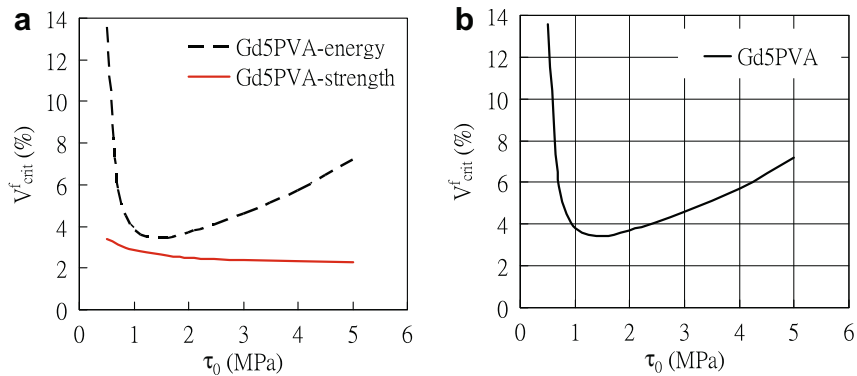


Fig. 5. Micromechanical model calculated V_{crit}^f as a function of τ_0 for strain-hardening (control) PVA-fiber cement determined by: (a) the energy and the strength criterion respectively and (b) the combined effect.

fiber (G_d5PVA) with surrounding cement matrix. Crack tip bridging by such fibers results in a high matrix cracking strength of 4.5 MPa [11,12]. Fig. 5 shows V_{crit}^f as a function of τ_0 for the control PVA fi-

ber (G_d5PVA) cement system. As can be seen, the energy criterion overwhelms the strength criterion and governs the composite behavior. Due to the strong hydrophilic tendency of the surface

of PVA fiber, a high interface frictional bond is usually found, e.g. τ_0 can be as high as 5.7 ± 0.6 MPa [7]. Therefore, increase of PVA fiber (G_d 5PVA) strength is expected to greatly reduce V_{crit}^f . In contrast, increase of PVA fiber (G_d 5PVA) length will not improve the composite ductility much due to high τ_0 in the PVA fiber (G_d 5PVA) cement system (similar to that shown in Fig. 4 for PP fiber at high τ_0).

An alternative route would be to alter the chemical bonding as illustrated in Fig. 6. The micromechanical parameters used in calculating the V_{crit}^f plots for G_d 2PVA fiber system are identical with the control PVA system (G_d 5PVA), except that the chemical bond was lowered from 5 to 2 J/m² and the matrix cracking strength was reduced from 4.5 MPa to 3.5 MPa due to the lower G_d [11,12]. As can be seen, lowering G_d greatly shifts the energy curve down at all τ_0 and the strength curve is also dragged down mainly caused by the reduction of σ_0 (from 6.5 to 5 MPa allowed by the

reduction in σ_{fc}). In the case of G_d 2PVA, the combined curve indicates that lowering G_d is an effective way to reduce the V_{crit}^f at all τ_0 for achieving tensile strain-hardening behavior.

In the previous discussion, focus has been placed on altering the fiber and interface properties in order to shift the V_{crit}^f curve down. In fact, matrix tailoring, e.g. manipulating the pre-existing flaw size distribution and the matrix fracture toughness, can be the third element in this micromechanics-based composite optimization [12]. For a brittle matrix composite, the stress to initiate a crack from a pre-existing defect, the cracking strength σ_{fc} is largely determined by the largest flaw normal to the maximum principle tensile stress. The maximum fiber bridging stress σ_0 imposes a lower bound on the critical flaw size such that only flaws larger than this critical size can be activated and contribute to multiple cracking. Insufficient number of such flaws in the matrix causes

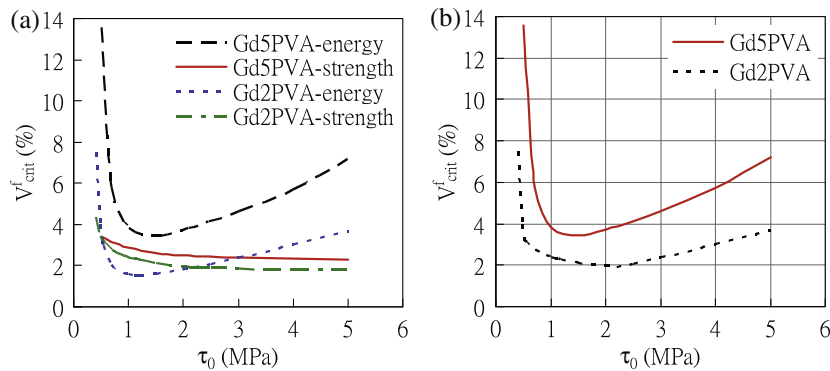


Fig. 6. Effect of interface chemical bond on V_{crit}^f determined by: (a) the energy and the strength criterion respectively and (b) the combined effect.

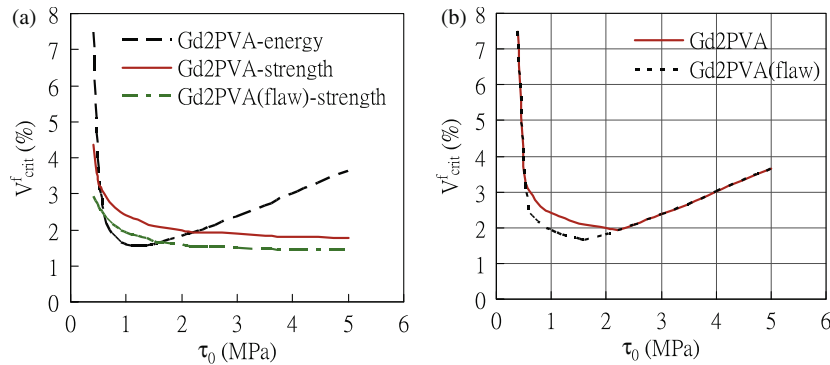


Fig. 7. Effect of planting artificial flaws in matrix on V_{crit}^f determined by: (a) the energy and the strength criterion respectively and (b) the combined effect.

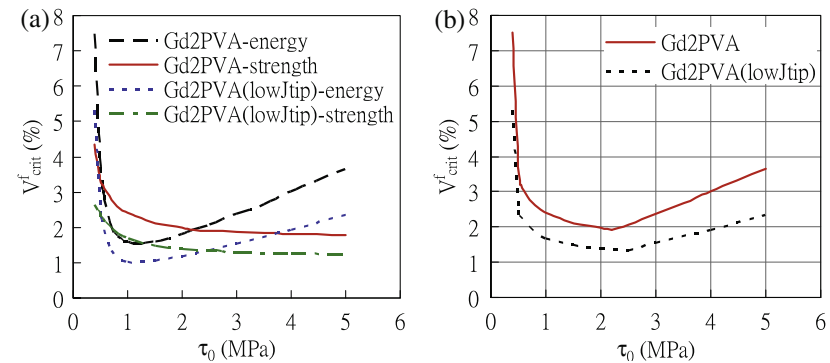


Fig. 8. Effect of matrix toughness on V_{crit}^f determined by: (a) the energy and the strength criterion respectively and (b) the combined effect.

Table 3
Micromechanical parameters used in calculating $\sigma(\delta)$ curve of PVA-fiber cement.

	Fiber parameters					Interface parameters					Matrix parameters	Model results	
	V_f (vol.%)	d_f (μm)	L_f (mm)	E_f (GPa)	σ_{fu} (MPa)	G_d (J/m^2)	τ_0 (MPa)	β	f	f'	E_m (GPa)	J'_b (J/m)	σ_0 (MPa)
Virgin PVA	2	39	8	42.8	1070	5.29	2.93	2.92	0.5	0.32	20	8.8* (15)	5.6* (6.5)
1.2% Coated PVA	2	39	8	42.8	1070	1.61	1.11	1.15	0.5	0.32	20	43.0* (15)	5.1* (5)

* Required minimum J'_b and σ_0 for tensile strain-hardening behavior of PVA-fiber cement (see Section. 3).

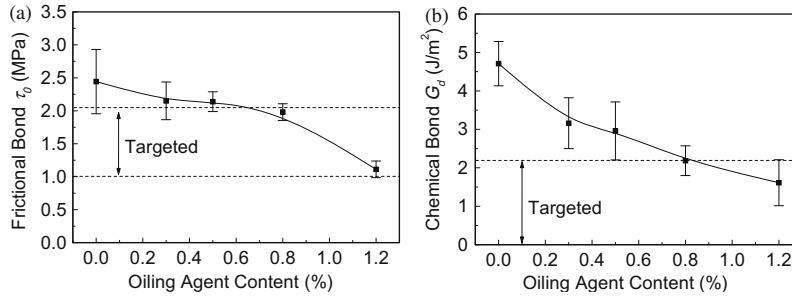


Fig. 9. Effect of coating content on interface: (a) frictional bond and (b) chemical bond (after [11]).

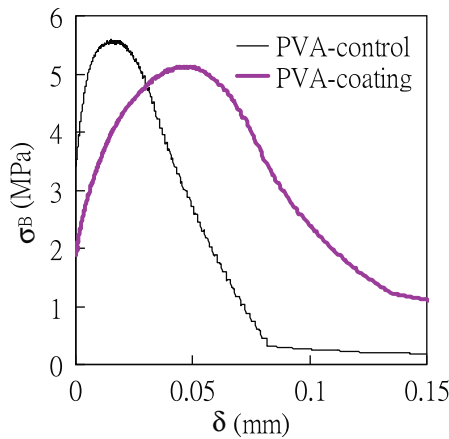


Fig. 10. Effect of interface tailoring on predicted $\sigma(\delta)$ curve of PVA-fiber cement.

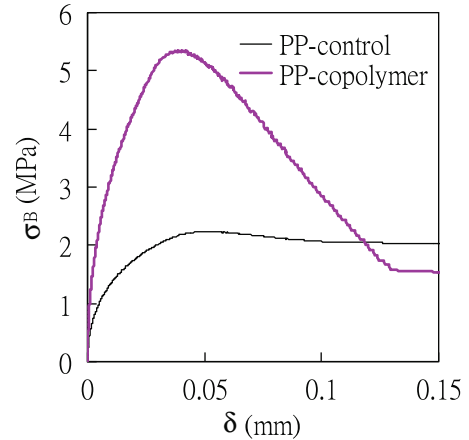


Fig. 12. Effect of fiber and interface tailoring (high tenacity copolymer fiber) on $\sigma(\delta)$ curve of PP fiber cement.

unsaturated multiple cracking, and therefore a larger PSH strength index (σ_0/σ_{fc}) is required for saturated multiple cracking. A practical approach to controlling the pre-existing flaws, i.e. introducing artificial defects with prescribed size distribution, has been demonstrated and proved an efficient way to achieving robust strain-hardening behavior [13]. Fig. 7 displays the effect of introducing artificial flaws into matrix. All micromechanical parameters are identical with G_d 2PVA except that a smaller performance index

(σ_0/σ_{fc} is set to be 1.15 instead of 1.45) was used to reflect the higher probability of reaching saturated multiple cracking with emplacement of artificial flaws. Note that the performance index J'_b/J_{tip} remains the same because implantation of artificial defects does not affect the propagation of cracks. Therefore, the same energy curves can be expected for the G_d 2PVA (flaw) case in Fig. 7a. As can be seen, strength curve shifts down and the combined curve

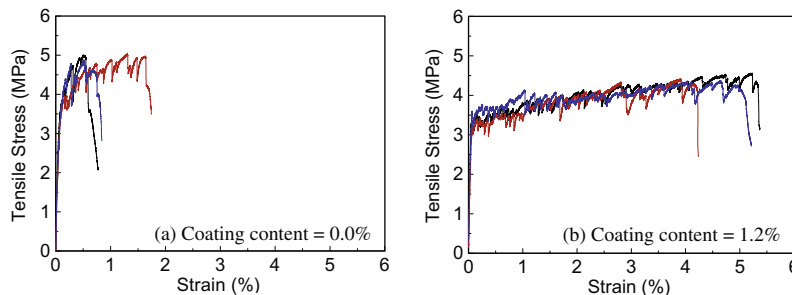


Fig. 11. Effect of interface tailoring on composite tensile stress–strain behavior of PVA-fiber cement – three curves in each plot represents three repeatable test results (after [11]).

in Fig. 7b indicates that the minimum V_{crit}^f can be further lowered due to intentionally implanting of artificial defects into the matrix.

Another approach to matrix modification relates the change of matrix toughness J_{tip} . Fig. 8 illustrates the effect of matrix toughness on the V_{crit}^f plot. The micromechanical parameters are identical

with G_d2PVA except a lower J_{tip} ($5 \rightarrow 3.3 \text{ J/m}^2$) and σ_{fc} ($3.5 \rightarrow 2.5 \text{ MPa}$) were used. Same performance index ($J_b = 3J_{tip}$ and $\sigma_0 = 1.45\sigma_{fc}$) were used to calculate the strength and energy curve in Fig. 8a. It is clear that both the energy and strength curves as well as the combined curve shift down at all range of τ_0 . It can

Table 4
Micromechanical parameters used in calculating $\sigma(\delta)$ curve of PP fiber cement.

	Fiber parameters					Interface parameters					Model results	Matrix parameters	
	V_f (vol.%)	d_f (μm)	L_f (mm)	E_f (GPa)	σ_{fu} (MPa)	G_d (J/m^2)	τ_0 (MPa)	β	f	f'		E_m (GPa)	J_b (J/m^2)
ControlPP	2	11	8	11.6	400	0	0.22	0.005	0.39	0.1	20	24.8 (15)	2.2 (5)
CopolymerPP	2	11	8	11.6	749	0	1.02	0.005	0.39	0.1	20	54.6 (15)	5.3 (5)

* Required minimum J_b and σ_0 for tensile strain-hardening behavior of PP fiber cement (see Section. 3).

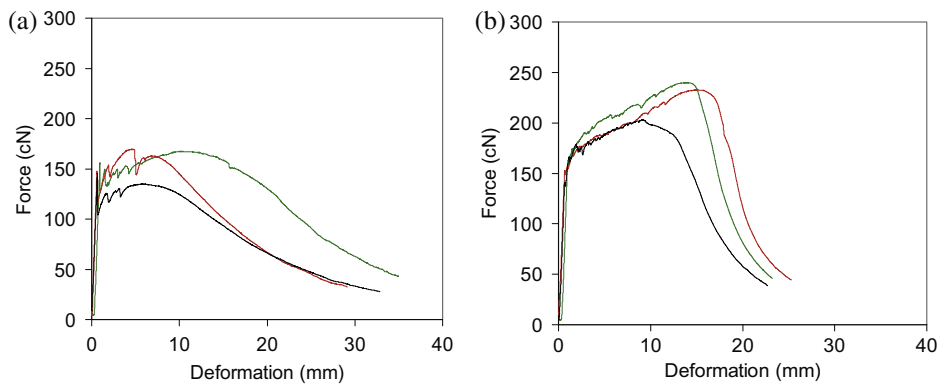


Fig. 13. Three-point bending test load-deformation curve of fiber cement reinforced by 1.5 wt.%. (a) ordinary high tenacity PP fiber and (b) copolymer fiber with polyolefinic in the sheath – three curves in each plot represents three repeatable test results (after [8]).

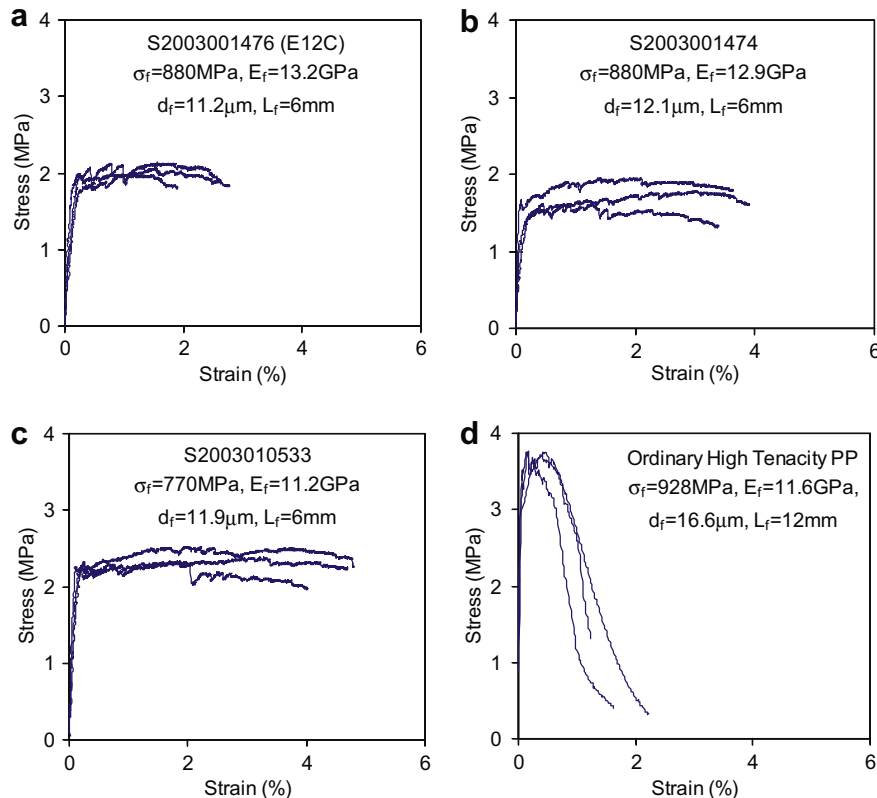


Fig. 14. Tensile stress–strain curves of PP fiber cement. (a–c) Tensile strain-hardening behavior of PP copolymer fiber cement, and (d) tension-softening behavior of ordinary high tenacity PP fiber cement.

Table 5

Mechanical and geometric properties of three copolymer PP fibers and ordinary high tenacity PP fibers.

	σ_f (MPa)	E_f (GPa)	ε_f (%)	L_f (mm)	d_f (μm)
Copolymer PP (a) S2003001476 (E12 C)	880	13.2	17.6	6	11.2
Copolymer PP (b) S2003001474	880	12.9	25.7	6	12.1
Copolymer PP (c) S2003010533	770	11.2	19.1	6	11.9
Ordinary high tenacity PP	928	11.6	N/A	12	16.6

Table 6Mix design of PP fiber cement (unit: kg/m^3).

Cement	Fly ash	Water	SP	PP fiber
412	1154	363	6.6	18

be concluded that low matrix toughness is beneficial for multiple cracking. However, excessively low matrix toughness may lead to low compressive strength, and is generally not desirable.

4. Examples of composite optimization

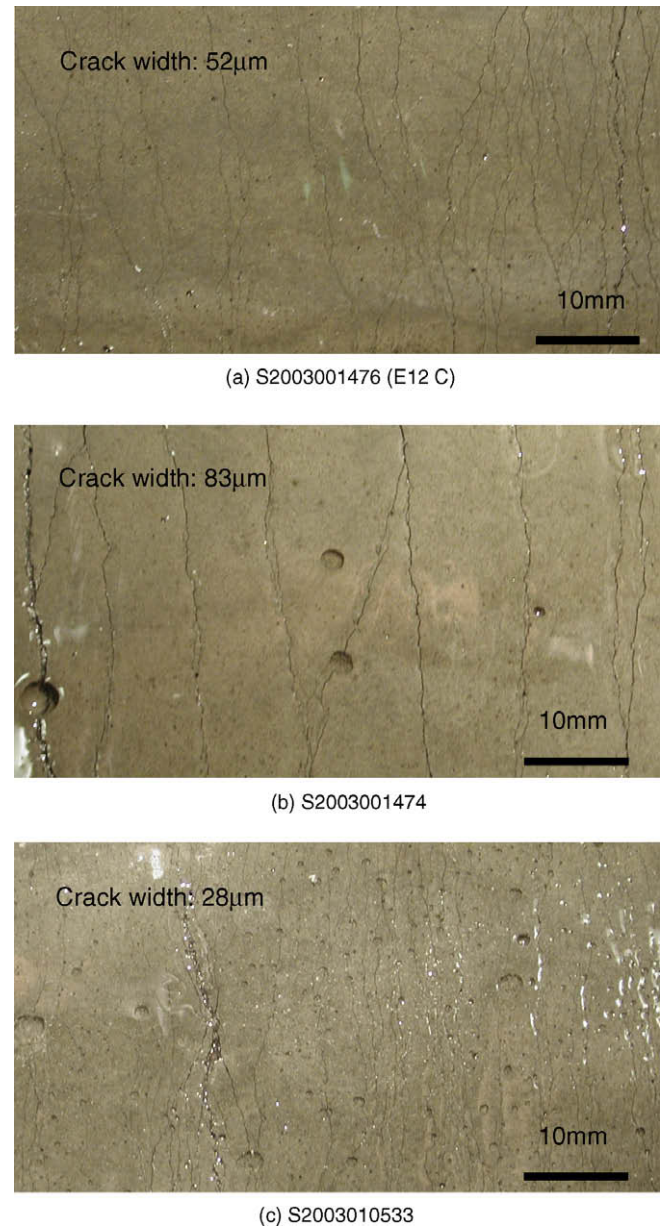
The previous section illustrates the concepts of composite optimization by means of micromechanics-based strain-hardening model. Through the guidance of the model, composite tensile strain-hardening behavior can be achieved by adopting minimum amount of fiber with properly tailored fiber, matrix, and interface. In this section, examples are given to demonstrate the practice of composite optimization of PVA and PP fiber reinforced cement composites, respectively.

As depicted in Fig. 5b, virgin PVA fiber has strong interfacial chemical and frictional bonds, which demands high amount of fiber (4–6 vol.%) in order to achieve strain-hardening behavior. From micromechanics model (Fig. 6b), lowering chemical and frictional bonds are effective approaches to reduce V_{crit}^f . This can be realized by modifying the surface properties of PVA fiber. It is known that the strong interfacial bonds of PVA fiber are introduced by its hydrophilic surface. Therefore, a feasible way to reduce the hydrophilic tendency would be coating a thin layer of oiling agent onto the surface of PVA fiber [11]. Fig. 9 shows the effect of surface coating on interfacial bonding. As can be seen, both the chemical and frictional bonds drop significantly with increase amount of surface oiling (wt.%). When the oil content reaches 0.8–1.2%, the τ_0 and G_d drops to 1–2 MPa and about $2 \text{ J}/\text{m}^2$, respectively. According to Fig. 6b– G_d 2PVA, such interface property values are optimal for design of a ductile fiber cement with 2 vol.% fiber content.

Fig. 10 displays the predicted σ – δ curves of virgin PVA fiber (control) as well as surface-coated (1.2 wt.% oiling agent) PVA fiber based on the micromechanics model. The micromechanical parameters used in calculating the $\sigma(\delta)$ are listed in Table 3. Meanwhile, the resulting complementary energy and peak bridging strength of $\sigma(\delta)$ are also reported in Table 3. As can be seen, J_b^0 and σ_0 of the control PVA system do not satisfy the strain-hardening criteria. The surface-coated PVA system; however, can meet both the strength and energy requirement. The tensile stress–strain curve of control PVA and 1.2% surface-coated PVA fiber reinforced cement composites are shown in Fig. 11, respectively. As can be seen, significant improvement in terms of tensile ductility was found in the surface-coated PVA fiber system, which validates the effectiveness of micromechanics model and demonstrates the feasibility of composite optimization.

For the PP fiber system, increase of fiber strength along with higher frictional bond τ_0 could be an efficient way to improve composite ductility (Fig. 3b). The weak bonding of ordinary PP fibers can be attributed to their low surface energy (hydrophobic charac-

ter) and low surface roughness. It has been reported that surface treatment with plasma can increase the surface energy of hydrophobic fiber, and therefore interfacial bonding [14]. Another approach would be to produce PP fibers whose sheath layer composition, and thus surface properties, differs from their core. A high tenacity copolymer PP fiber produced by Redco was used in this study [8]. Fig. 12 shows the predicted σ – δ curves of control PP fiber system along with the copolymer PP fiber system. The micromechanical parameters for these two systems are listed in Table 4. As can be seen, the strength and τ_0 are greatly improved

**Fig. 15.** Crack pattern of tensile strain-hardening PP copolymer fiber cement.

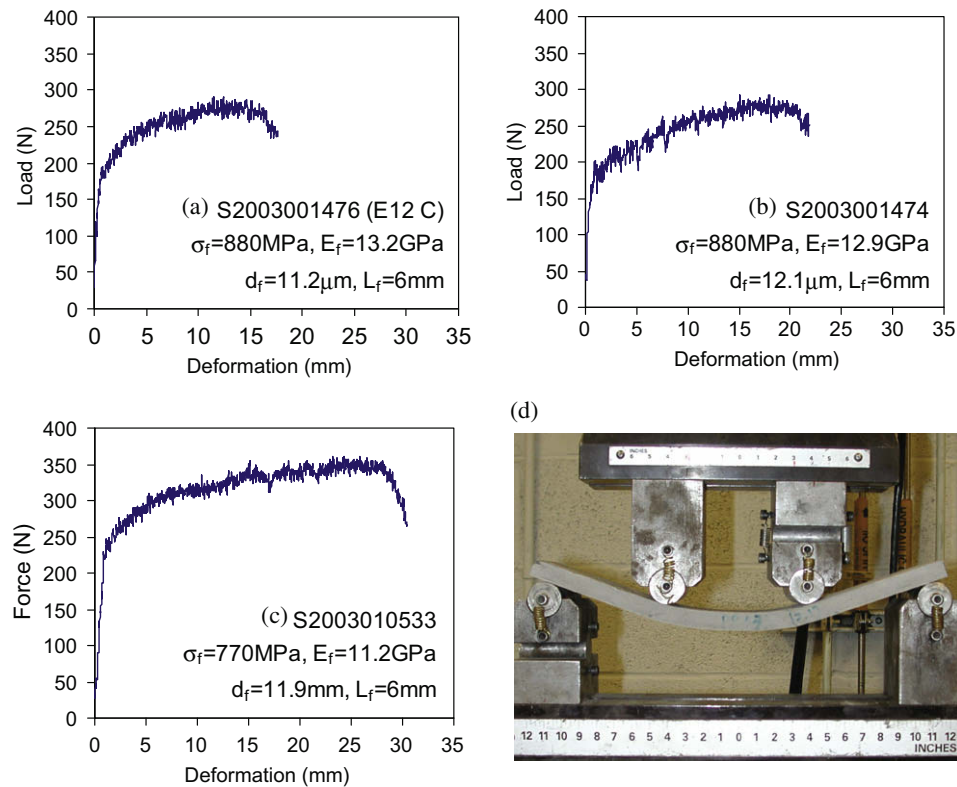


Fig. 16. Four point bending load-deformation behavior of PP copolymer fiber cement.

and the copolymer system satisfy the strain-hardening criterion at 2 vol.% fiber fraction, which is consistent with the prediction in Fig. 3b. Bending tests of this copolymer PP fiber cement sheets show significant differences in composite response. The most distinctive difference is the unstable growth of an edge crack under bending load when the ordinary PP is used. When the copolymer PP fiber is used in the same fiber content, no such unstable crack was observed, and the crack width is much smaller [8], characteristic of a strain-hardening composite. The contrasting flexural curves are shown in Fig. 13.

Based on the guidance of the micromechanical model, strain-hardening PP fiber cement incorporating 2 vol.% copolymer PP fiber has been successfully developed recently. Fig. 14 shows the tensile stress-strain curve of four PP fiber cements, in which (a)–(c) adopted high tenacity copolymer PP fibers and (d) incorporated an ordinary high tenacity PP fiber. The ordinary high tenacity PP fiber was used as control. The three high tenacity copolymer PP fibers used were also produced by Redco. The mechanical and geometric properties of those PP fibers can be found in Table 5. Notice that a longer fiber length was intentionally chosen for the ordinary high tenacity PP fiber. The analysis in Fig. 4 indicates that longer fiber length is beneficial for fibers with low frictional bond, which is the case of ordinary high tenacity PP fiber. Therefore, use of longer fiber gives a better chance for the tensile strain-hardening behavior in ordinary high tenacity PP fiber cement. However, longer fiber length can greatly reduce the workability and introduce poor fiber dispersion. In this study, an ordinary high tenacity PP fiber with 12 mm in length was used in order to obtain decent workability and fiber dispersion. The mix proportion of PP fiber cement is shown in Table 6.

Despite the use of long fiber, ordinary high tenacity PP fiber cement still shows tension-softening behavior as illustrated in Fig. 14d. For the copolymer PP fiber cements; however, strain-hardening behavior with great improvement in the tensile ductility (2–5%) was obvious. It is interesting to show that copolymer PP (c)

fiber cement has the highest composite tensile strength as well as the tensile strain capacity despite the fact that the copolymer PP (c) fiber itself has the lowest fiber strength among those high tenacity PP fibers. This may be attributed to a stronger interfacial bonding within copolymer PP (c) fiber cement resulting in a higher bridging strength and a larger complementary energy. Fig. 15 displays the crack pattern of copolymer PP fiber cements. Uniformly distributed and saturated cracks were found in all three copolymer PP fiber cements. From the crack spacing and crack width, it suggests that copolymer PP (c) has the strongest interfacial bonds and copolymer PP (b) has the weakest interfacial bonds. This observation further confirms and explains the composite behavior as indicated above. Therefore, fiber strength is not the only factor that dominates the composite behavior. Control of the synergistic interaction between fiber, matrix, and interface is the key to optimize composite behavior. Fig. 16 shows the bending behavior of those copolymer PP fibers. Again, copolymer PP (c) has the best bending ductility and bending strength.

5. Conclusions

Micromechanics-based model linking characteristics of composite constituents to composite tensile strain-hardening behavior can be used for systematic optimization of composite tensile ductility while minimizing the fiber content. This approach is holistic, simultaneously taking into account the interacting effects of fiber, matrix, and interface properties on composite response. Due to the large number of micromechanical parameters (13) governing composite response, this micromechanics-based approach for composite optimization is much more efficient than the traditional empirical trial-and-error approach.

It is shown that in general, the strength and energy criteria must be considered to ensure adequate initiation of multiple cracks, and that cracks initiated propagate in the flat steady-state

cracking mode, in order to achieve saturated multiple cracking so that a robust ductile composite is assured. In the case of (control) PP fiber cement, the critical fiber content to achieve strain-hardening is governed by both the strength and energy criteria, depending on the interfacial frictional bond strength. In the case of (strong) PP fiber cement, the critical fiber content is controlled only by the strength criterion. In the case of (control) PVA-fiber cement; however, the critical fiber content is dominated by the energy criterion.

The micromechanical-based model can be translated into specific guidance for composite component tailoring. Parametric studies in this paper reveal that enhanced fiber strength may benefit composite ductility at high interfacial friction condition. In contrast, increase of fiber length promotes composite multiple-cracking behavior primarily at low τ_0 region. Lowering interface chemical bond usually decreases the critical fiber volume for achieving tensile strain-hardening. Matrix tailoring, including intentionally implanting artificial defects and reduction of matrix toughness, can be an alternative for composition optimization.

The micromechanics-based model suggests very different engineering strategies for different types of fiber systems. In the case of PVA fiber, surface treatment leading to a reduction of bond properties is beneficial to composite ductility. Specifically, G_d and τ_0 values of 1.6 J/m^2 and 1.1 MPa leads to a composite with high tensile ductility at fiber content of 2 vol.%. In contrast, increase in frictional bonding greatly enhances composite performance when PP fiber is utilized. Here, τ_0 of 1.0 MPa for an enhanced fiber strength of 749 MPa is recommended. Experimental data show significant improvements in composite ductility when these fibers are properly tailored, thus confirming the effectiveness of the micromechanics approach. Although applied to two specific fiber types in this paper, the theoretical tools developed are applicable to a wide range of fiber types and brittle matrix types.

References

- [1] Kim PJ. Micromechanics based durability study of lightweight thin sheet fiber reinforced cement composites, in department of civil and environmental engineering. Ann Arbor: University of Michigan; 1999. p. 486.
- [2] Li VC, Leung CKY. Steady state and multiple cracking of short random fiber composites. *J Eng Mech-ASCE* 1992;118(11):2246–64.
- [3] Lin Z, Kanda T, Li VC. On interface property characterization and performance of fiber-reinforced cementitious composites. *J Concr Sci Eng* 1999(1):173–84.
- [4] Yang E, Wang S, Yang Y, Li VC. Fiber-bridging constitutive law of engineered cementitious composites. *J Adv Coner Technol* 2008;6(1):181–93.
- [5] Marshall DB, Cox BN. A J-integral method for calculating steady-state matrix cracking stresses in composites. *Mech Mater* 1988(8):127–33.
- [6] Kanda T. Design of engineered cementitious composites for ductile seismic resistant elements, in department of civil and environmental engineering. Ann Arbor: University of Michigan; 1998.
- [7] Wu C. Micromechanical tailoring of PVA-ECC for structural applications in departmental of civil and environmental engineering. Ann Arbor: University of Michigan; 2001. p. 238.
- [8] De Lhoneux B, Kalbskopf R, Kim P, Li V, Lin Z, Vidts D, et al. Development of high tenacity polypropylene fibres for cementitious composites. In: Proceedings of the JCI international workshop on ductile fiber reinforced cementitious composites (DFRCC)—application and evaluation, Takayama, Japan; 2002.
- [9] Stang H, Mobasher B, Shah SP. Quantitative damage characterization in polypropylene fiber reinforced concrete. *Cem Concr Res* 1990;20(4):540–58.
- [10] Takashima H, Miyagai K, Hashida T, Li VC. A design approach for the mechanical properties of polypropylene discontinuous fiber reinforced cementitious composites by extrusion molding. *J Eng Fract Mechs* 2003;70:853–70.
- [11] Li VC, Wu C, Wang S, Ogawa A, Saito T. Interface tailoring for strain-hardening PVA-ECC. *ACI Mater J* 2002;99(5):463–72.
- [12] Wang S. Micromechanics based matrix design for engineered cementitious composites, in departmental of civil and environmental engineering. Ann Arbor: University of Michigan; 2005.
- [13] Li VC, Wang S. Microstructure variability and macroscopic composite properties of high performance fiber reinforced cementitious composites. *Probab Eng Mech* 2006;21(3):201–6.
- [14] Li VC, Wu HC, Chan YW. Effect of plasma treatment of polyethylene fibers on interface and cementitious composite properties. *Cem Concr Compos* 1996;18(4):223–37.